Supplementary Material

Fluorinated Cardo-based Polyimide Membranes for Helium Extraction from Natural Gas

ShanYang[1], Mengxin Li[1], Jiawang Li[1], Yan Liu[1], Xin Zhang[1], Deqing Shi[1,*] Xinliang Liu[1,2], Ming Wang[1,*], Yingfei Hou[1,*]

[1] *State Key Laboratory of Heavy Oil Processing, China University of Petroleum (East China), Qingdao 266580, China*

[2] *Advanced Chemical Engineering and Energy Materials Research Center, China University of Petroleum (East China), Qingdao 266580, China*

[*] Corresponding author.

E-mail address: *wmalfred@upc.edu.cn* (Ming Wang)

E-mail address: *houyf@upc.edu.cn* (Yingfei Hou)

Materials.

All monomers and reagents were procured from commercial suppliers and used without further purification unless specified. 6FDA (purity > 98%), 4,4'-(9H-fluorene-9,9-diyl)dianiline (Cardo, purity > 99%), 4,4'-(9H-fluorene-9,9-diyl)bis(2-methylaniline) (purity > 98%), 9,9-bis(4-amino-3-chlorophenyl)fluorene(purity > 98%), and 4,4'-(9H-fluorene-9,9-diyl)bis(2-fluoroaniline) (purity > 98%) were purchased from Shanghai Macklin Biochemical Technology Co., Ltd. (China) and dried under vacuum prior to use. *m*-Cresol was obtained from Sinopharm Chemical Reagent Co., Ltd. (China) and used as received. Ethanol (purity > 99.7%), chloroform ($CHCl_3$, purity > 99.0%), and tetrahydrofuran (THF, HPLC grade, purity > 99.5%) were sourced from Shanghai Macklin Biochemical Technology Co., Ltd.

Characterization Methods.

The polyimide or polyimide membranes were characterized through multiple analytical techniques. ^{1}H and ^{13}C NMR spectra were recorded in $CDCl_3$-d_6 using 400 MHz NMR spectrometer (Bruker AV 400 MHz). FT-IR spectroscopy was performed on a Bruker VERTEX70 spectrometer in attenuated total reflection mode with 4 cm^{-1} resolution, scanning from 3000 to 200 cm^{-1} for functional group analysis. Molecular weight distribution was analyzed by gel permeation chromatography (GPC, Shimadzu CBM-20A control module) using THF as eluent and polystyrene standards. Optical transmittance of the membranes was measured by ultraviolet-visible spectroscopy (UV-Vis, Shimadzu UV-2700). The back surface structure of the copolyimide membrane was characterized by atom force microscope (AFM, Shimadzu SPM-9700) and

scanning electron microscopy (SEM, JSM-7610Fplus). Thermal stability of the membranes was evaluated by differential scanning calorimetry (DSC, Shimadzu DSC-60plush) under nitrogen atmosphere at a heating rate of 5°C/min. The *d*-spacing was determined through WAXD measurements conducted on an X'Pert PRO MPD system with field-emission electron probe, utilizing Cu-Kα radiation (2θ range: 5°-50°). Mechanical properties were evaluated using an HY-0580 microcomputer-controlled electronic universal material testing machine in accordance with Chinese National Standard GB/T 1040.3-2006, employing a crosshead speed of 5 mm/min. The hydrophobicity of the membranes was analyzed using a contact angle goniometer (DSA 30, KRÜSS GmbH, Germany) via the sessile drop method with a droplet volume of 2 μL. The measured contact angles were corrected for surface roughness based on Wenzel's equation ($\cos\theta_m = r\cdot\cos\theta_Y$, where θ_m represents the apparent contact angle, θ_Y denotes the intrinsic Young's contact angle, and r is the roughness factor defined as the ratio of actual surface area to geometrically smooth surface area).

Molecular simulation

MD simulations were performed using the COMPASS II force field. Energy minimization was conducted via the Smart Minimizer method with a convergence threshold of 0.001 kcal/mol. Electrostatic interactions were computed using the Ewald summation method, while van der Waals interactions were treated with the atom-based option using a cutoff distance of 12.5 Å. Four simulation cells were constructed using the Amorphous Cell module. For each cell, sequential procedures including geometry optimization, annealing, and NPT dynamics were executed to ensure complete

structural relaxation of the polymer. Subsequent NVT dynamics simulations were carried out. Fractional free volume (FFV) was determined according to Eq. (S1).

$$FFV = \frac{V_f}{V_f + V_0} \quad \text{(S1)}$$

The equation defined V_f as the free volume of the simulated system and V_0 as the occupied volume of the molecular structure.

NMR and FT-IR spectroscopic characterization of four polyimide membranes.

6FDA-Cardo (**M_0**). Yellow fibrous solid, yield 89.19%. ^{1}H NMR (400 MHz, Chloroform-d_6) δ 8.00(d, J=8.0 Hz, 2H), 7.92(s, 2H), 7.81(dd, J=16.2, 7.7 Hz, 4H), 7.45(d, J=7.5 Hz, 2H), 7.38(d, J=8.7 Hz, 6H), 7.30(d, J = 8.0 Hz, 6H). ^{13}C NMR (101 MHz, Chloroform-d) δ 165.97(d, J=12.4 Hz), 150.22, 145.81, 140.19, 139.14, 135.92, 132.50(d, J=30.0 Hz), 129.96, 129.02, 127.99(d, J=7.0 Hz), 126.28(d, J=13.5 Hz), 125.31, 124.11, 120.37, 65.05. FT-IR (ATR, v, cm^{-1}): 1780 (C=O, asymmetric stretching), 1720 (C=O, asymmetric stretching), 1380 (C-N, stretching vibration), 1250-1100 (C-F, stretching vibration).

6FDA-Cardo-CH_3 (**M_1**). Yellow fibrous solid, yield 93.51%. ^{1}H NMR (400 MHz, Chloroform-d_6) δ 8.01 (d, J=8.0 Hz, 2H), 7.91(s, 2H), 7.86(d, J=7.9 Hz, 2H), 7.79(d, J=7.5 Hz, 2H), 7.45(d, J=7.5 Hz, 2H), 7.40(t, J=7.3 Hz, 2H), 7.32(t, J=7.4 Hz, 2H), 7.24 -7.16(m, 4H), 7.06(d, J=8.3 Hz, 2H), 2.10 (s, 6H). ^{13}C NMR (101 MHz, Chloroform-d) δ 166.06(d, J=16.0 Hz), 150.22, 147.06, 140.18, 139.09, 136.26, 132.73(d, J=30.6 Hz), 129.21-123.26(m), 65.04, 18.36. FT-IR (ATR, v, cm^{-1}): 1780 (C=O, asymmetric stretching), 1720 (C=O, asymmetric stretchin), 1380 (C-N, stretching vibration), 1250-1100 (C-F, stretching vibration).

6FDA-Cardo-Cl (**M_2**). Light yellow fibrous solid, yield 82.98%. ^{1}H NMR (400 MHz, Chloroform-d_6) δ 8.03 (d, J=8.1 Hz, 2H), 7.95(d, J=3.4 Hz, 2H), 7.83 (dd, J=17.0, 7.3 Hz, 4H), 7.43 (d, J=7.8 Hz, 4H), 7.39-7.31(m, 6H), 7.27(d, J=1.8 Hz, 1H), 7.25(s, 1H). ^{13}C NMR (101 MHz, Chloroform-d) δ 165.27(d, J=15.7 Hz), 148.56(d, J=38.7 Hz), 140.16, 139.24, 133.81-131.71(m), 130.35, 129.61, 128.72-127.30(m), 126.19, 124.36, 120.69, 64.68. FT-IR (ATR, v, cm^{-1}): 1780 (C=O, asymmetric stretching), 1720 (C=O, asymmetric stretchin), 1380 (C-N, stretching vibration), 1250-1100 (C-F, C-Cl, stretching vibration).

6FDA-Cardo-F (**M_3**). Yellowish-brown fibrous solid, yield 94.90%. ^{1}H NMR (400 MHz, Chloroform-d_6) δ 8.02(d, J=8.1 Hz, 2H), 7.95(s, 2H), 7.86-7.78(m, 4H), 7.43(t, J=6.6 Hz, 4H), 7.35(t, J=7.4 Hz, 2H), 7.28 (s, 1H), 7.24(s, 1H), 7.23-7.19(m, 2H), 7.14-7.06(m, 2H). ^{13}C NMR (101 MHz, Chloroform-d) δ 165.13 (d, J=12.7 Hz), 156.13, 148.93, 140.15, 139.22, 132.65(d, J=29.2 Hz), 129.44, 128.44(d, J=14.6 Hz), 126.18, 125.48, 124.46(d, J=27.8 Hz), 120.63, 117.64, 116.52(d, J=21.2 Hz), 64.89. FT-IR (ATR, v, cm^{-1}): 1780 (C=O, asymmetric stretching), 1720 (C=O, asymmetric stretchin), 1380 (C-N, stretching vibration), 1250-1100 (C-F, stretching vibration).

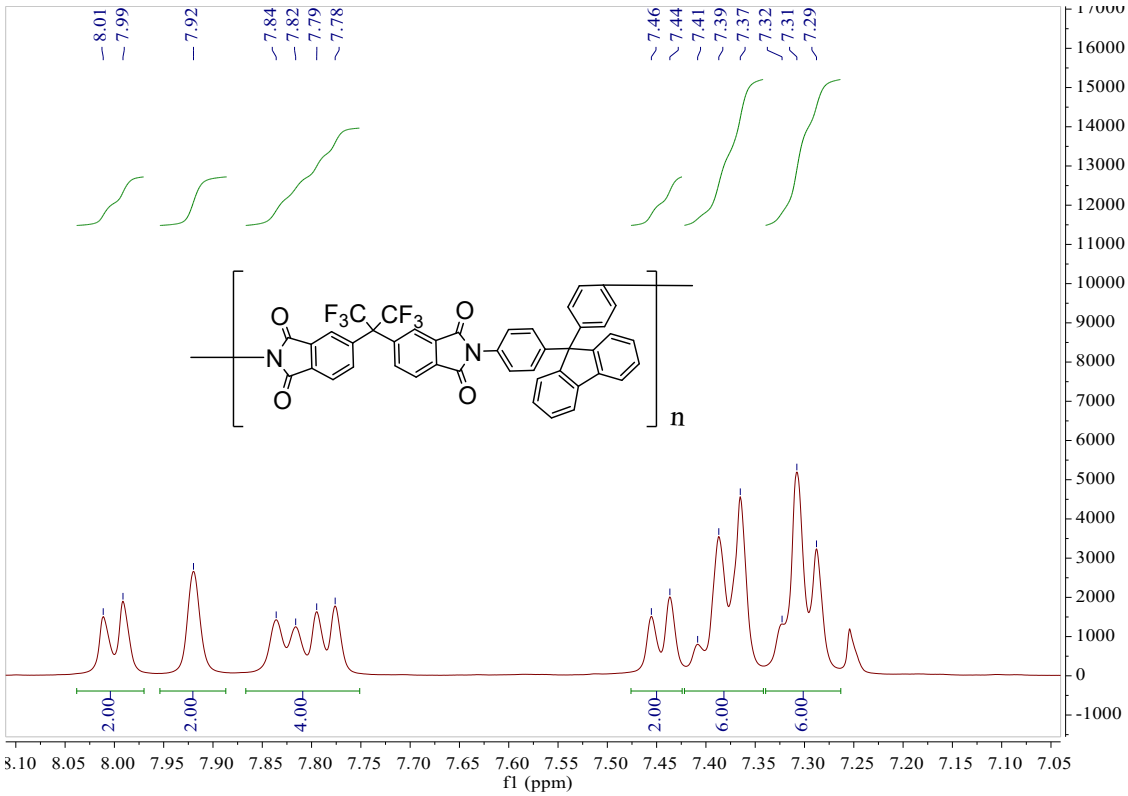

Figure S1. [1]H NMR spectrum of **M_0**.

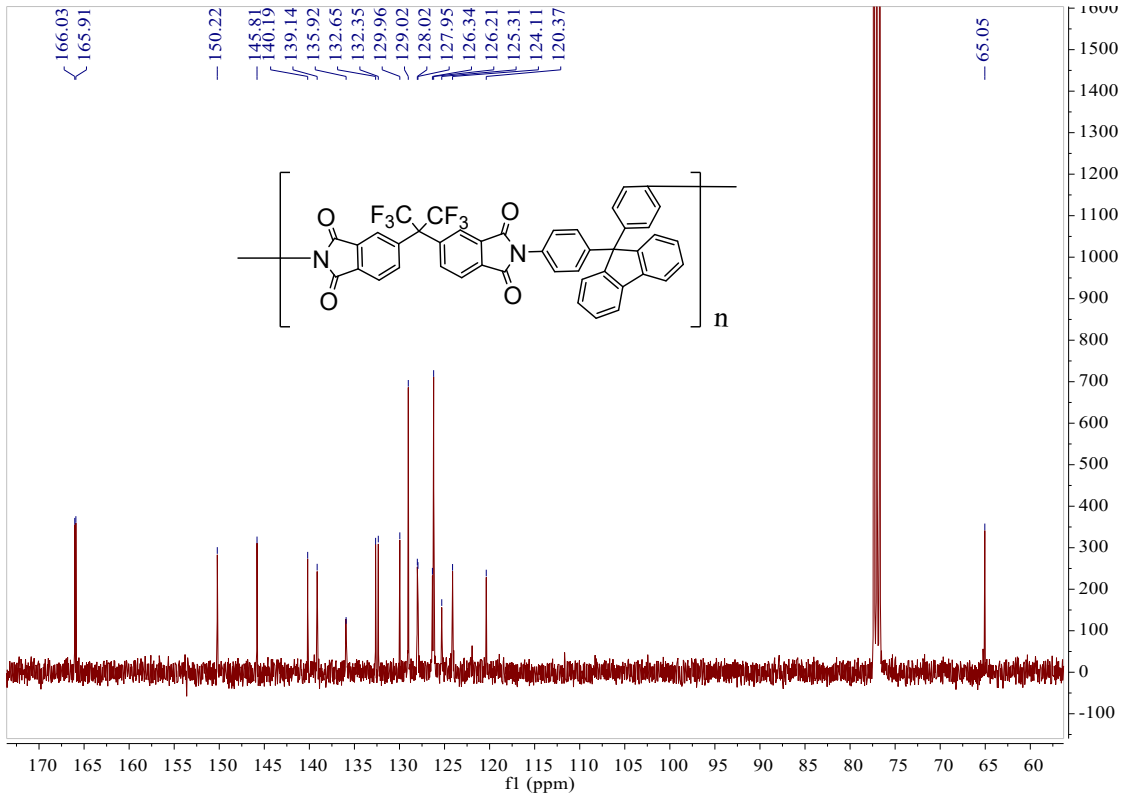

Figure S2. [13]CNMR spectrum of **M_0**.

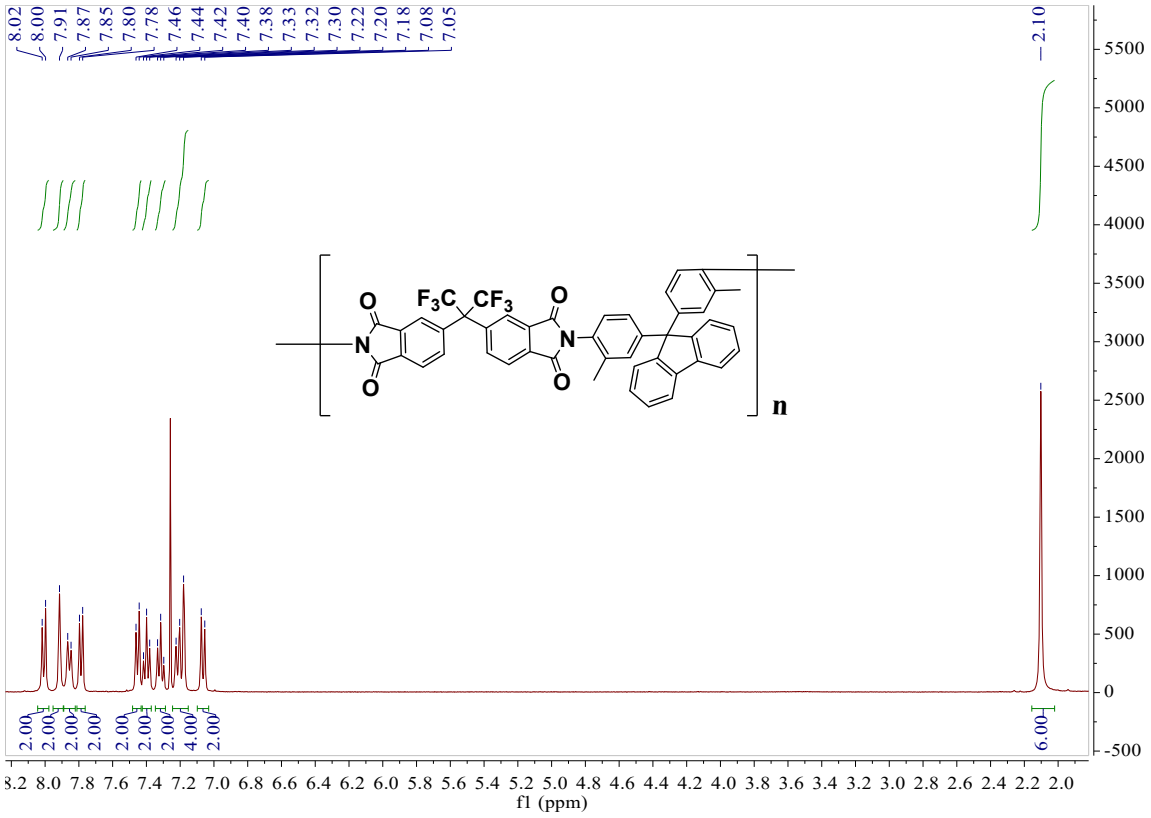

Figure S3. ^{1}H NMR spectrum of $\mathbf{M_1}$.

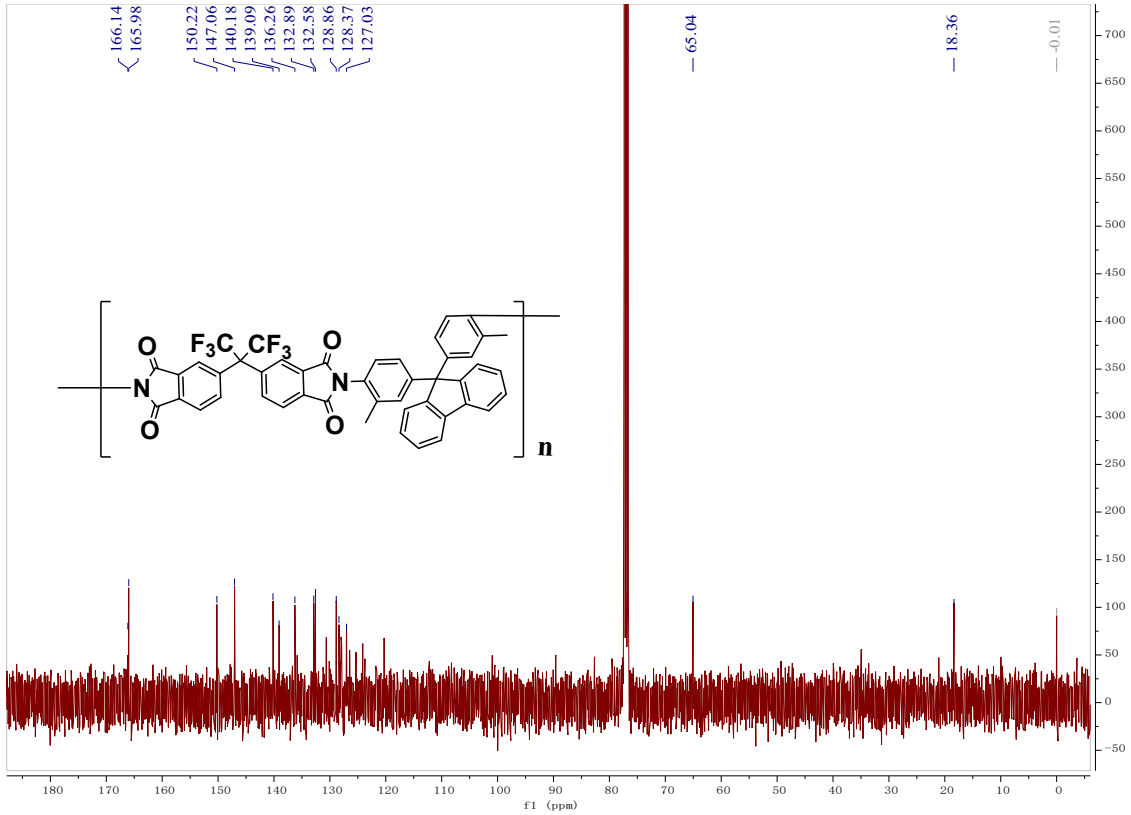

Figure S4. ^{13}CNMR spectrum of $\mathbf{M_1}$.

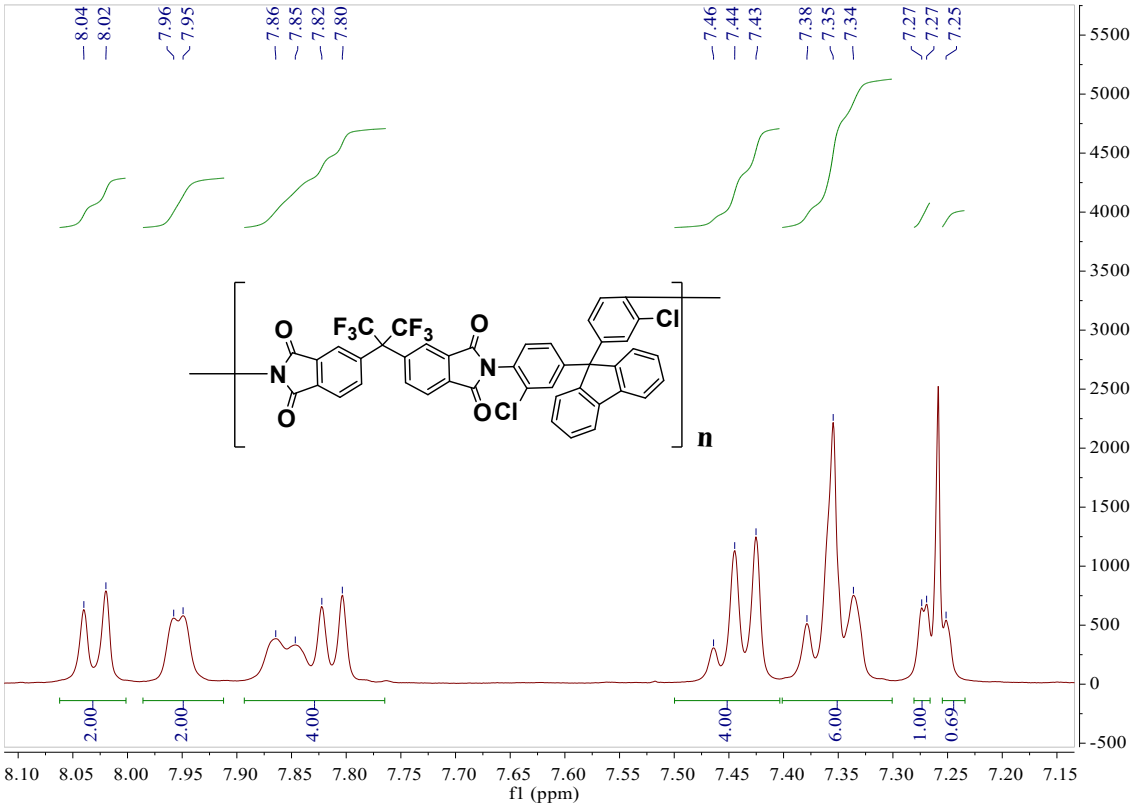

Figure S5. ^{1}H NMR spectrum of $\mathbf{M_2}$.

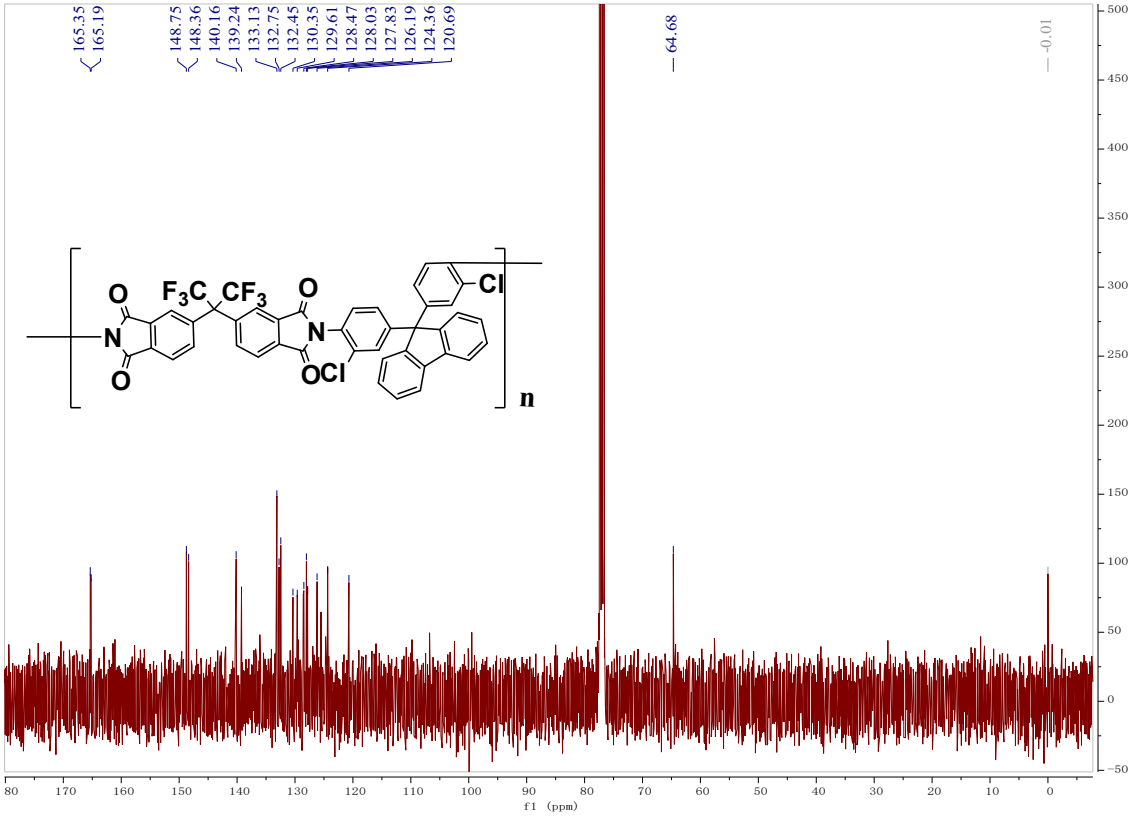

Figure S6. ^{13}CNMR spectrum of $\mathbf{M_2}$.

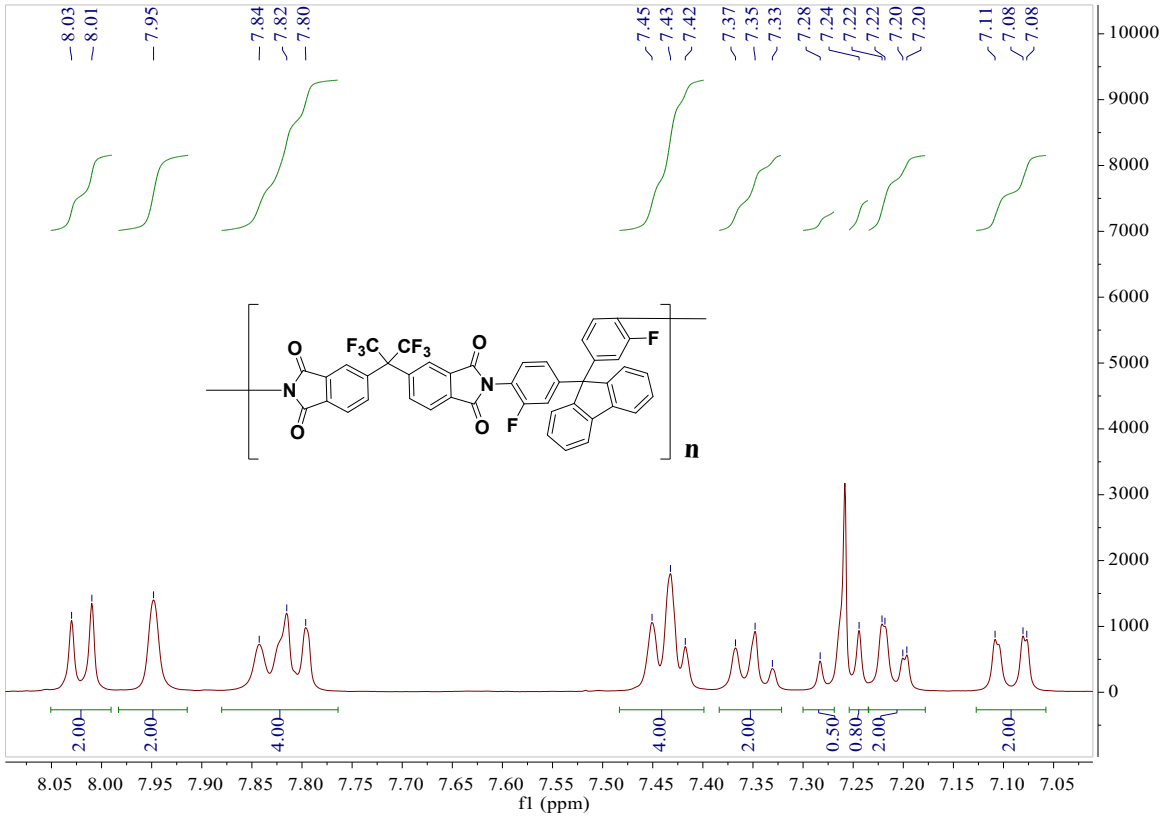

Figure S7. ^{1}H NMR spectrum of $\mathbf{M_3}$.

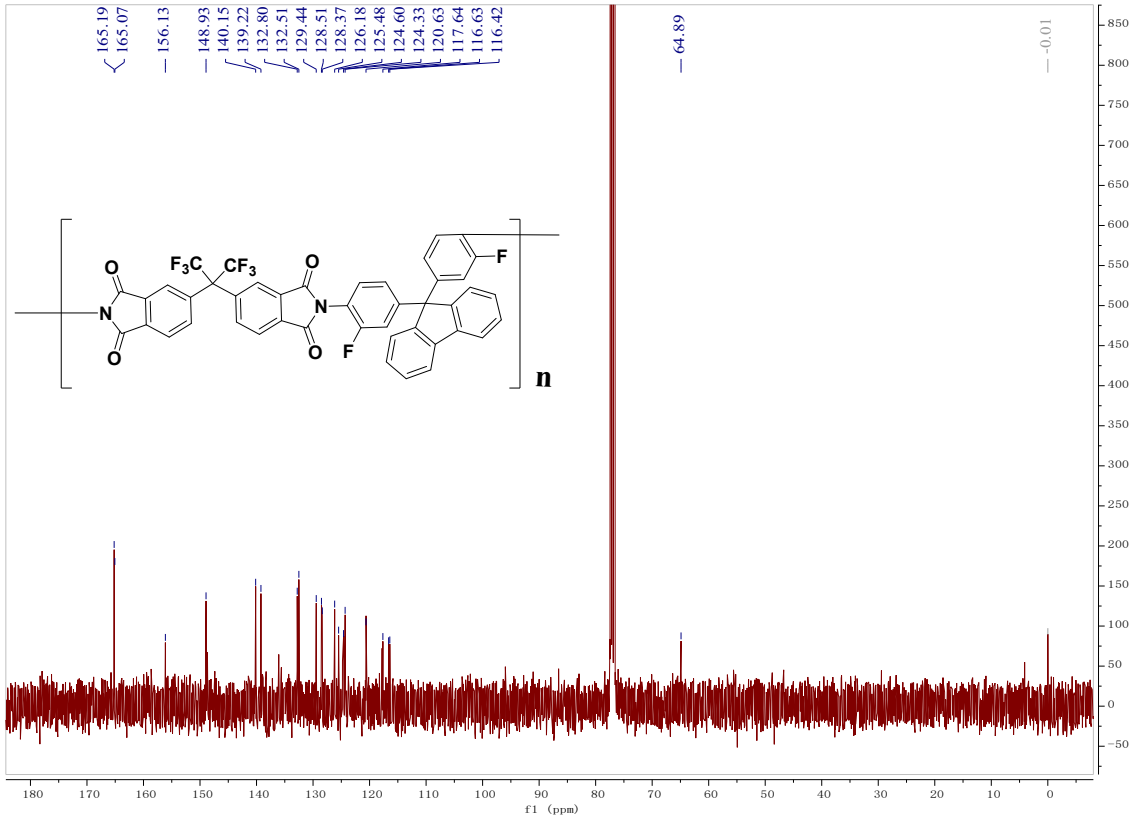

Figure S8. ^{13}CNMR spectrum of $\mathbf{M_3}$.

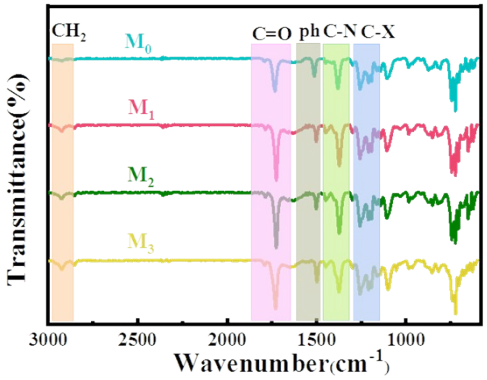

Figure S9. FT-IR spectra of the polyimide membranes.

Table S1. General properties of polyimide membranes.

polymer	M_w (g/mol)	M_n (g/mol)	PDI (M_w/M_n)	Tg (°C)	2θ(deg)	*d*-spacing (Å)
M_0	225780	105996	2.13	446.22	15.17/20.75	5.83/4.28
M_1	236873	115625	2.05	352.62	15.06/20.68	5.87/4.29
M_2	125075	63482	1.97	329.32	15.04/20.68	5.89/4.29
M_3	183137	82527	2.22	251.52	15.13/20.75	5.85/4.28

Table S2. Pure gas testing and ideal selectivity for **M_0-M_3**.

ID	Permeability of pure gas (Barrer)					Ideal selectivity	
	He	H_2	CO_2	N_2	CH_4	P_{He}/P_{CH4}	P_{He}/P_{N2}
M_0	118.99	23.41	48.14	6.89	3.97	29.98	17.28
M_1	248.90	68.00	123.54	14.67	9.17	27.13	16.96
M_2	263.56	71.99	146.08	16.27	10.03	26.27	16.20
M_3	158.10	36.46	61.28	11.32	6.20	25.48	13.96

Table S3. Mixed gas testing and actual selectivity for $\mathbf{M_0}$-$\mathbf{M_3}$.

ID	Binary He/CH_4 mixture			Binary He/N_2 mixture		
	P_{He}/Barrer	P_{CH4}/Barrer	$\alpha_{He/CH4}$	P_{He}/Barrer	P_{N2}/Barrer	$\alpha_{He/N2}$
$\mathbf{M_0}$	142.63	9.21	15.49	120.52	7.73	15.60
$\mathbf{M_1}$	263.15	16.22	16.22	213.32	13.80	15.48
$\mathbf{M_2}$	272.90	18.84	14.49	225.94	12.45	18.20
$\mathbf{M_3}$	154.13	6.63	23.26	155.88	7.06	22.10

Table S4. Gas permeability of $\mathbf{M_1}$-$\mathbf{M_3}$ ranging from 30 to 80 °C.

ID	T/°C	Binary He/CH_4 mixture			Binary He/N_2 mixture		
		P_{He}/Barrer	P_{CH4}/Barrer	$\alpha_{He/CH4}$	P_{He}/Barrer	P_{N2}/Barrer	$\alpha_{He/N2}$
$\mathbf{M_0}$	30	135.25	8.15	16.60	120.53	7.17	16.80
	40	159.11	9.61	16.55	133.16	7.57	17.60
	50	181.96	11.21	16.24	147.66	7.49	19.72
	60	210.21	13.17	15.96	170.78	8.40	20.33
	70	242.80	15.55	15.62	187.36	8.86	21.14
	80	276.12	19.72	14.00	208.14	9.51	21.88
$\mathbf{M_1}$	30	252.78	14.30	17.68	213.77	13.37	15.99
	40	281.51	15.71	17.92	235.02	14.16	16.59
	50	323.64	16.47	19.65	268.96	15.30	17.58
	60	362.40	17.89	20.26	288.57	16.54	17.44
	70	393.66	20.60	19.11	326.60	18.15	17.99
	80	414.91	24.06	17.24	368.72	18.61	19.81
$\mathbf{M_2}$	30	261.03	16.36	15.95	240.10	13.35	17.98
	40	290.08	17.61	16.47	247.67	13.56	18.26
	50	330.97	18.27	18.12	279.18	13.61	20.51
	60	370.67	19.29	19.21	312.43	13.43	23.26
	70	422.83	22.40	18.88	347.59	13.19	26.36
	80	457.10	24.75	18.47	379.62	13.53	28.06
$\mathbf{M_3}$	30	153.81	6.54	23.54	155.65	6.97	22.33

	40	192.71	8.18	23.57	166.32	6.77	24.56
	50	214.14	8.77	24.42	183.22	6.77	27.06
	60	242.68	10.31	23.54	206.77	6.69	30.93
	70	275.01	13.62	20.19	234.94	7.07	33.23
	80	308.79	15.56	19.85	256.76	7.02	36.57

Table S5. Gas permeability of M_1-M_3 ranging from 0.3 to 0.8 MPa.

ID	P/MPa	Binary He/CH_4 mixture			Binary He/N_2 mixture		
		P_{He}/Barrer	P_{CH4}/Barrer	$\alpha_{He/CH4}$	P_{He}/Barrer	P_{N2}/Barrer	$\alpha_{He/N2}$
M_0	0.3	136.68	8.41	16.26	116.28	5.87	19.81
	0.4	122.99	7.86	15.66	106.688	4.76	22.40
	0.5	118.29	8.45	14.00	103.718	4.05	25.58
	0.6	115.78	8.84	13.09	100.62	3.55	28.34
	0.7	113.24	9.27	12.22	98.36	3.44	28.60
	0.8	112.78	9.62	11.72	98.00	3.33	29.46
M_1	0.3	253.36	15.64	16.20	213.77	13.37	15.99
	0.4	223.14	13.98	15.96	202.32	10.20	19.83
	0.5	209.77	13.68	15.33	193.72	9.63	20.12
	0.6	196.61	13.47	14.60	187.20	8.45	22.15
	0.7	188.12	13.87	13.56	181.29	8.05	22.53
	0.8	182.24	14.03	12.99	178.02	6.74	26.40
M_2	0.3	258.28	17.90	14.43	239.70	12.18	19.68
	0.4	222.79	16.03	13.90	219.00	9.74	22.49
	0.5	212.68	15.76	13.49	208.90	8.08	25.85
	0.6	201.39	15.44	13.04	203.18	6.97	29.15
	0.7	194.94	15.23	12.80	196.08	6.32	31.03
	0.8	188.72	14.96	12.62	192.53	5.84	32.97

	0.3	153.81	6.54	23.54	155.72	6.96	22.37
	0.4	143.00	6.33	22.58	138.14	5.33	25.90
	0.5	139.66	6.53	21.40	133.79	4.32	30.97
M_3	0.6	135.78	6.57	20.68	128.48	3.82	33.64
	0.7	128.93	6.78	19.03	127.11	3.37	37.70
	0.8	125.89	7.00	18.00	125.06	3.09	40.53

Table S6. Polymer density, free volume fraction and binding energy of He and CH_4 in polymers.

polymers	**density (g/cm^3)**	**FFV**	**CED (MJ/cm^3)**	**Eint (kcal/mol)**		**Diffusion coefficient (D, 10^{-6} cm^2/s)**	
				He	**CH_4**	**He**	**CH_4**
M_0	1.28	25.12	356.2±0.36	-2.58	-133.29	46.746	10.256
M_1	1.24	26.26	317.1±0.33	-2.97	-144.83	53.720	12.380
M_2	1.29	27.88	357.6±0.34	-2.71	-156.00	52.045	16.116
M_3	1.31	25.39	353.7±0.30	-3.08	-137.74	64.311	9.982